Differential Inhibition of Class I and Class II 5-Enolpyruvylshikimate-3-phosphate Synthases by Tetrahedral Reaction Intermediate Analogues[†,‡]

Todd Funke,[§,||] Martha L. Healy-Fried,[§,||] Huijong Han,[§] David G. Alberg,[⊥] Paul A. Bartlett,[⊥] and Ernst Schönbrunn*[,§,▽]

Department of Medicinal Chemistry, University of Kansas, Lawrence, Kansas 66045, and Department of Chemistry, University of California, Berkeley, California 94720-1460

Received June 4, 2007; Revised Manuscript Received September 9, 2007

ABSTRACT: The shikimate pathway enzyme 5-enolpyruvylshikimate-3-phosphate synthase (EPSP synthase or EPSPS) is best known as the target of the herbicide glyphosate. EPSPS is also considered an attractive target for the development of novel antibiotics since the pathogenicity of many microorganisms depends on the functionality of the shikimate pathway. Here, we have investigated the inhibitory potency of stable fluorinated or phosphonate-based analogues of the tetrahedral reaction intermediate (TI) in a parallel study utilizing class I (glyphosate-sensitive) and class II (glyphosate-tolerant) EPSPS. The (*R*)-difluoromethyl and (*R*)-phosphonate analogues of the TI are the most potent inhibitors of EPSPS described to date. However, we found that class II EPSPS are up to 400 times less sensitive to inhibition by these TI analogues. X-ray crystallographic data revealed that the conformational changes of active site residues observed upon inhibitor binding to the representative class I EPSPS from *Escherichia coli* do not occur in the prototypical class II enzyme from *Agrobacterium* sp. strain CP4. It appears that because the active sites of class II EPSPS do not possess the flexibility to accommodate these TI analogues, the analogues themselves undergo conformational changes, resulting in less favorable inhibitory properties. Since pathogenic microorganisms such as *Staphylococcus aureus* utilize class II EPSPS, we conclude that the rational design of novel EPSPS inhibitors with potential as broad-spectrum antibiotics should be based on the active site structures of class II EPSP synthases.

The enzyme 5-enolpyruvylshikimate-3-phosphate synthase (EPSP synthase or EPSPS;[1] EC 2.5.1.19) catalyzes the sixth step of the shikimate pathway. The product of the shikimate pathway, chorismate, serves as a starting material for the biosynthesis of essential compounds including the aromatic amino acids and cofactors such as ubiquinone, vitamin K, and folate in plants, fungi, and microorganisms (*1*−*3*), while mammals obtain necessary aromatic compounds from their diets. A variety of evidence suggests that EPSPS and other shikimate pathway enzymes represent enticing drug targets. The deletion of the gene encoding EPSPS has been shown to result in attenuated virulence in *Staphylococcus aureus*, *Streptococcus pneumoniae*, and *Bordetella bronchiseptica* (*4*−*6*). Many organisms, including *Mycobacterium tuberculosis*, *Pseudamonas aeruginosa*, *Vibrio cholerae*, and *Yersinia pestis*, require the production of chorismate-derived siderophores for pathogenicity (*7*, *8*). Further, glyphosate has been shown to inhibit the in vitro growth of apicomplexan parasites including *Toxoplasma gondii*, *Plasmodium falciparum*, and *Cryptosporidium parvum* (*9*).

As the molecular target of glyphosate (the active ingredient in Roundup herbicide), EPSPS has been the subject of extensive investigation (*10*, *11*). While glyphosate has proven to be a potent inhibitor of EPSPS from plants and *Escherichia coli*, several glyphosate-tolerant forms of EPSPS have been identified (*12*−*16*). Glyphosate-tolerant EPSPS isolated from organisms including *S. aureus*, *S. pneumoniae*, *Pseudomonas* sp. strain PG2982, and *Agrobacterium* sp. strain CP4 are termed class II enzymes, while the plant and *E. coli* enzymes are considered class I enzymes (*16*−*18*). The molecular basis for glyphosate tolerance in the prototypical class II enzyme *Agrobacterium* sp. strain CP4 EPSPS has been elucidated recently (*19*).

Although glyphosate restricts the growth of apicomplexan parasites, its antibiotic properties are poor, and pathogens such as *S. pneumoniae* and *S. aureus* have class II EPSPS which present unsuitable targets for glyphosate (*16*, *17*). Thus, the effective targeting of microbial EPSPS requires new strategies toward the design of novel inhibitors. In

[†] This work was supported by the National Institutes of Health (Grant 1R01 GM70633-02).

[‡] The atomic coordinates and structure factors have been deposited in the Protein Data Bank (http://www.rcsb.org/), codes 2PQ9 for *E. coli* EPSPS liganded with 2F-TI, 2PQB for CP4 EPSPS liganded with 2F-TI, 2PQC for CP4 EPSPS liganded with RP-TI, and 2PQD for Ala100Gly CP4 EPSPS liganded with 2F-TI.

* To whom correspondence should be addressed. Phone: (813) 745-4703. Fax: (813) 745-6748. E-mail: ernst.schonbrunn@moffitt.org.

[§] University of Kansas.

[||] These authors contributed equally to this work.

[⊥] University of California.

[▽] Current address: Drug Discovery Program, H. Lee Moffitt Cancer Research Institute, Tampa, FL 33612.

[1] Abbreviations: EPSP synthase or EPSPS, 5-enolpyruvylshikimate-3-phosphate synthase; TI, tetrahedral reaction intermediate; *S. aureus*, *Staphylococcus aureus*; *E. coli*, *Escherichia coli*; CP4, *Agrobacterium* sp. strain CP4; PEP, phosphoenolpyruvate; S3P, shikimate 3-phosphate; RP-TI, (*R*)-phosphonate TI analogue; SP-TI, (*S*)-phosphonate TI analogue; 2F-TI, (*R*)-difluoromethyl TI analogue; TIAs, TI analogues.

10.1021/bi701095u CCC: $37.00
Published on Web 10/25/2007

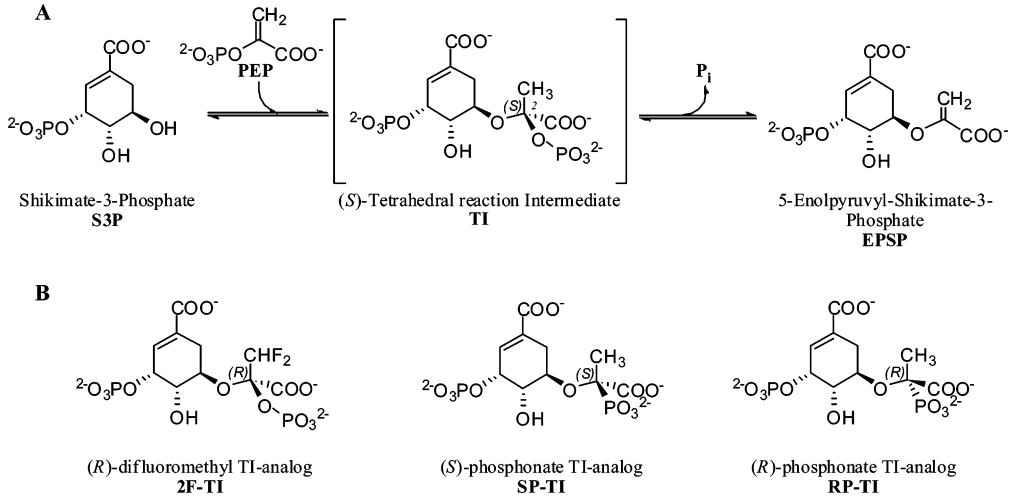

FIGURE 1: (A) Reaction catalyzed by EPSPS. **(B)** TI analogues studied in this work.

particular, detailed atomic-level information is needed about inhibitors other than glyphosate.

EPSPS transfers the enolpyruvyl moiety of phosphoenolpyruvate (PEP) to the 5′-oxygen atom of shikimate 3-phosphate (S3P). The reaction proceeds through a tetrahedral reaction intermediate (TI) in which the two substrates are covalently linked (Figure 1a). Crystallographic and chemical studies using *E. coli* EPSPS demonstrated the 2-(*S*)-configuration of the TI (*20*, *21*). The mode of action of glyphosate on EPSPS is well understood (*22*, *23*), but intensive efforts to find a molecule better than glyphosate at inhibiting class I EPSPS have largely failed; only a few analogues of the TI have been identified as more potent inhibitors (*11*, *24*, *25*). The molecular modes of action of the (*R*)- and (*S*)-phosphonate TI analogues (RP-TI and SP-TI, respectively) on *E. coli* EPSPS were determined recently by X-ray crystallography and indicated that this enzyme may facilitate the tight binding of such inhibitors through conformational flexibility (*25*). Notably, inhibition studies on EPSPS have only been performed using class I enzymes (*11*, *24*). Here, we have investigated the molecular modes of action of RP-TI, SP-TI, and the (*R*)-difluoromethyl TI analogue (2F-TI) (Figure 1b) using class II EPSPSs from both *S. aureus* and *Agrobacterium* sp. strain CP4 in parallel with the class I EPSPS from *E. coli*. The results demonstrate that class II EPSPS are generally less susceptible to inhibition by these TI analogues. Crystallographic studies illuminate the basis for this discriminant inhibition.

EXPERIMENTAL PROCEDURES

Materials. S3P (triethylammonium salt) was synthesized and purified as previously described (*25*). Syntheses of the TI analogues (2F-TI, RP-TI, and SP-TI) were reported previously (*24*). PEP (potassium salt) and all other chemicals were purchased from Sigma (St. Louis, MO) unless otherwise noted. The Pierce (Rockford, IL) Coomassie Plus reagent with bovine serum albumin as a standard was used to determine protein concentrations. Wild type *E. coli* EPSPS (*15*), *Agrobacterium* sp. strain CP4 EPSPS (wild type and Ala100Gly mutant) (*19*), and wild-type *S. aureus* EPSPS (*16*) were overexpressed and purified as previously described.

Inhibition Kinetics. The kinetic properties of the EPSPS were examined using the malachite green phosphate-release assay (*26*). The protocol for kinetic assays has been changed slightly from that described previously (*25*) to facilitate higher throughput. Assays were conducted in 60 μL of 50 mM Na−HEPES, pH 7.5, 100 mM KCl, and 2 mM DTT, using 96-well microtiter plates. The reaction was started by the addition of enzyme, incubated at 25 °C, and stopped by addition of 140 μL of malachite green reagent after 20 min (*S. aureus* EPSPS) or 30 min (*E. coli*, wild-type CP4, and Ala100Gly CP4 EPSPS). After allowance of 10 min for color development, the change in optical density at 650 nm was measured with a SpectraMax 340PC plate reader (Molecular Devices, Sunnyvale, CA). The amount of product was determined by comparison to phosphate standards, and the enzyme activity is expressed as micromoles of phosphate produced per minute of reaction time per milligram of enzyme. The final concentration of the EPSPS was 1.4 nM for *E. coli*, 3.2 nM for both the wild-type CP4 and the Ala100Gly CP4, and 13 nM for *S. aureus*. To ensure that the results were directly comparable, the kinetic constants for *E. coli* EPSPS inhibition by RP-TI and SP-TI were redetermined using the plate-based assay.

Enzymatic activities at increasing S3P and varied inhibitor concentrations were recorded, and the data were fit to the Michaelis−Menten equation. K_i values for 2F-TI, RP-TI, and SP-TI were determined by linear regression of the replot of the $K_{m(obsd)}$ values versus the concentration of the inhibitor [I], where $K_{m(obsd)}$ is the observed Michaelis constant in the presence of inhibitor, K_m is the true Michaelis constant, and K_i is the inhibition constant (eq 1). Data evaluation for all kinetic experiments was performed with SigmaPlot (SPSS Science, Chicago, IL).

$$K_{m(obsd)} = \left(\frac{K_m}{K_i}\right)[I] + K_m \quad (1)$$

Crystallography. Highly purified enzymes were concentrated using Centricon 30 devices (Millipore, Billerica, MA) at 4 °C. Crystals were grown at 19 °C using the hanging-drop vapor diffusion method. *E. coli* EPSPS was crystallized in the presence of 10 mM 2F-TI using sodium formate crystallization conditions as previously described (*23*). Wild-type CP4 and Ala100Gly CP4 EPSPS were crystallized in the presence of 5 mM 2F-TI or 5 mM RP-TI using

Table 1: Summary of Data Collection and Structure Refinement[a]

data set	*E. coli*·2F-TI	CP4·2F-TI	CP4·RP-TI	CP4 (A100G)·2F-TI
space group	$P2_12_12_1$	$P2_1$	$P2_1$	$P2_1$
unit cell dimensions	$a = 58.2$ Å, $b = 85.1$ Å, $c = 87.6$ Å, $\alpha = \beta = \gamma = 90°$	$a = 63.4$ Å, $b = 45.0$ Å, $c = 77.6$ Å, $\alpha = \gamma = 90°$, $\beta = 106.1°$	$a = 63.0$ Å, $b = 45.0$ Å, $c = 77.3$ Å, $\alpha = \gamma = 90°$, $\beta = 106.3°$	$a = 62.8$ Å, $b = 44.9$ Å, $c = 77.1$ Å, $\alpha = \gamma = 90°$, $\beta = 106.4°$
protein atoms av *B* factor (Å^2)	3232	3260	3260	3259
	13.2	7.8	7.4	17.0
ligand atoms av *B* factor (Å^2)	28	28	25	28
	10.8	8.5	13.7	16.4
solvent molecules av *B* factor (Å^2)	443	483	506	447
	25.1	21.0	20.5	28.0
rmsd[b] (bonds) (Å)	0.011	0.011	0.011	0.011
rmsd (angles) (deg)	1.57	1.58	1.60	1.59
resolution range	15−1.6 (1.7−1.6)	10−1.8 (1.9−1.8)	15−1.6 (1.65−1.6)	15−1.77 (1.83−1.77)
no. of unique reflns	55458 (8807)	39118 (5810)	54614 (4686)	39870 (3885)
completeness (%)	95.4 (92.5)	99.6 (99.8)	98.9 (97.3)	98.2 (96.3)
$I/\sigma(I)$	24.4 (10.6)	13.0 (5.1)	14.7 (7.2)	26.0 (4.0)
R_{merge}[c] (%)	3.5 (8.8)	10.0 (19.7)	6.9 (12.5)	6.4 (35.6)
R_{cryst}[d] (%)	16.6	15.3	15.7	15.6
R_{free}[e] (%)	19.1	19.4	17.9	18.5

[a] Values in parentheses refer to the highest resolution shell. [b] rmsd = root-mean-square deviation from ideal values. [c] $R_{merge} = 100[\sum_h\sum_i|I_{hi} - I_h|/\sum_h I_{hi}]$, where h are unique reflection indices. [d] $R_{cryst} = 100[\sum|F_o - F_{model}|/\sum F_o]$, where F_o and F_{model} are observed and calculated structure factor amplitudes. [e] R_{free} is R_{cryst} calculated for randomly chosen unique reflections, which were excluded from the refinement (1109 for *E. coli*·2F-TI, 1173 for CP4·2F-TI, 1093 for CP4·RP-TI, and 1175 for CP4(A100G)·2F-TI).

ammonium sulfate crystallization conditions as previously described (*19*). X-ray diffraction data were recorded at −180 °C using the rotation method on single flash-frozen crystals [detector, *R*-axis IV^{++} image plate; X-rays, Cu Kα, focused by mirror optics; generator, Rigaku RU300 (MSC, The Woodlands, TX)]. The data were reduced with XDS (*27*) or HKL2000 (*28*). The program package CNS (*29*) was employed for phasing and refinement; model building was performed with *O* (*30*). The structures were solved by molecular replacement using wild-type *E. coli* EPSPS (PDB code 1G6S; *23*) or wild-type CP4 EPSPS (PDB code 2GG6; *19*) stripped of solvent molecules, ions, and ligands as search models. Refinement was performed using data to highest resolution with no σ cutoff applied. Several rounds of minimization, simulated annealing (2500 K starting temperature), and restrained individual *B*-factor refinement were carried out. Data collection and refinement statistics are summarized in Table 1. Figures 2−6 were drawn with Molscript (*31*), Bobscript (*32*), and Raster3D (*33*).

RESULTS AND DISCUSSION

Inhibition Kinetics. Steady-state kinetics employing the forward reaction with S3P and PEP as substrates were used to analyze the inhibitory actions of 2F-TI, RP-TI, and SP-TI on three enzymes: the class I EPSPS from *E. coli* and the class II EPSPS from both *S. aureus* and *Agrobacterium* sp. strain CP4. The data indicated that 2F-TI, RP-TI, and SP-TI are competitive inhibitors of the EPSPS reaction, irrespective of the enzyme's genetic origin (see Supporting Information Figures S1−S3). A very potent inhibitor of *E. coli* EPSPS ($K_i = 7.8$ nM), 2F-TI exhibits 4-fold and 8-fold decreased potency against *S. aureus* and CP4 EPSPS, respectively (Table 2). This trend is considerably more pronounced for EPSPS inhibition by the phosphonate diastereomers. RP-TI is a very potent inhibitor of *E. coli* EPSPS ($K_i = 3.9$ nM); however, it exhibits 120-fold and 460-fold less potency against *S. aureus* and CP4 EPSPS, respectively. SP-TI, a moderate inhibitor of the *E. coli* enzyme ($K_i = 760$ nM), is 16 times less active against the *S. aureus* enzyme ($K_i = 11$ μM) and essentially lacks inhibitory potency against the CP4 enzyme ($K_i = 76$ μM). While glyphosate sensitivity of the CP4 enzyme can be restored through a single-site mutation in the active site (Ala100Gly^{CP4}; *19*), the inhibition constants of the TI analogues are essentially the same for the Ala100Gly^{CP4} mutant as for wild-type CP4 EPSPS (data not shown). These findings indicate that class II enzymes such as *S. aureus* or CP4 EPSPS exhibit not only tolerance toward glyphosate but also considerably less susceptibility to inhibition by analogues of the TI.

Table 2: K_i Values (nM) for the Inhibition of EPSPS by TI Analogues

	2F-TI	RP-TI	SP-TI
E. coli	7.8 ± 0.5	3.9 ± 0.6	760 ± 200
CP4	63 ± 15	1800 ± 600	76000 ± 9000
S. aureus	30 ± 6	450 ± 70	11000 ± 2000

Molecular Modes of Action. The structure of the TI was previously determined in complex with a mutant *E. coli* EPSPS enzyme (Asp313Ala) (Figure 2) (*20*). In the *E. coli* and CP4 wild-type enzymes, the side chain of this aspartate (Asp313$^{E.coli}$/Asp326^{CP4}) establishes hydrogen bonds to the 4-OH and 5-OH of S3P, but is not part of the glyphosate or PEP binding site (*19*, *23*). For the TI analogues studied here and in our previous work (*25*), this side chain is too far away (>3.2 Å) and improperly oriented to interact efficiently with the moieties mimicking the PEP portion of the TI. Therefore, it is unlikely to influence the conformation of the TI, and thus, we refer to this conformation of the molecule as the "genuine" TI of the *E. coli* enzyme.

Interactions with 2F-TI. The *E. coli* and CP4 enzymes were cocrystallized with 2F-TI, and the structures were determined at 1.6 and 1.8 Å resolution, respectively (Table 1, Figures 2 and 4). The electron-dense difluoro moiety of 2F-TI induces a large conformational change of the side chain of Glu341 in *E. coli* EPSPS, but the conformation of 2F-TI and its interactions with active site residues are otherwise similar to those observed for the genuine TI (Figure 2). In

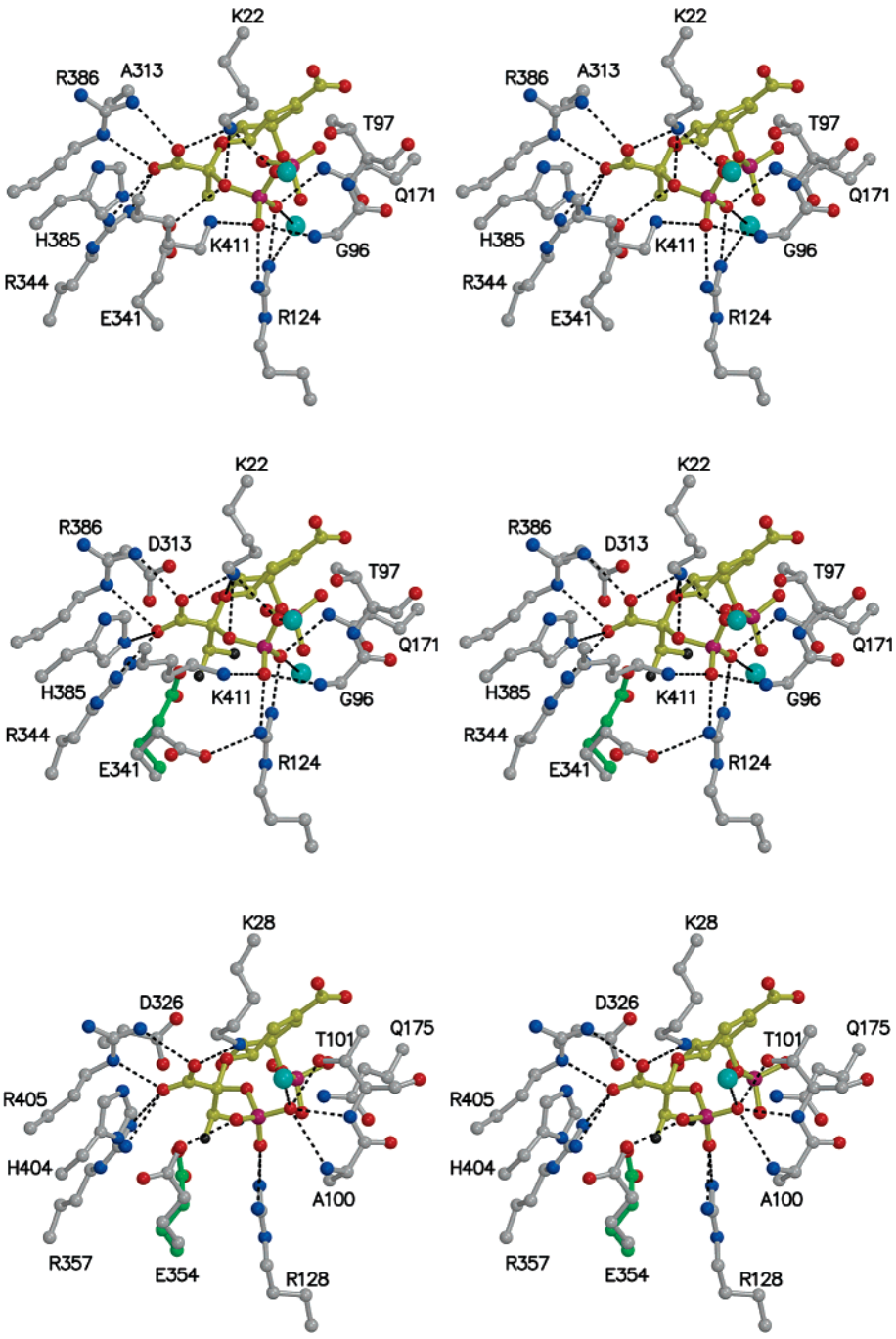

FIGURE 2: Interaction of 2F-TI with EPSPS (stereoview). Top: Genuine TI (shown in yellow) bound to *E. coli* EPSPS (PDB code 1Q36; *20*). Middle: 2F-TI binding to *E. coli* EPSPS induces a large conformational change of E341. Bottom: 2F-TI binding to CP4 EPSPS induces only a slight conformational change of E354 (=E341$^{E.coli}$). The residues shown in green display the conformations found in the respective binary complexes with S3P. Black dotted lines indicate polar interactions. The cyan spheres denote water molecules.

contrast, upon binding to the CP4 enzyme, the side chain of Glu354^{CP4} (=Glu341$^{E.coli}$) shifts only slightly away from 2F-TI, while the analogue itself undergoes a substantial conformational change, particularly around the *C*2-phosphate moiety (Figure 2). We tested whether this conformational change of the 2F-TI molecule in the CP4 enzyme is caused by the presence of Ala100^{CP4} (=Gly96$^{E.coli}$), known to induce structural changes in the glyphosate molecule (*19*). The X-ray structure of the Ala100Gly mutant CP4 enzyme in complex with 2F-TI revealed the same inhibitor conformation as observed with wild-type CP4 EPSPS (Figure S4). The side chain of Thr101^{CP4} protrudes into the site occupied by the phosphate group of 2F-TI when bound to the *E. coli* enzyme, and it thus appears that Thr101^{CP4}, not Ala100^{CP4}, is responsible for the rotation of the 2F-TI phosphate group in the CP4 enzyme. In *E. coli* EPSPS, the corresponding residue, Thr97$^{E.coli}$, is located further away from the phosphate group due to different ϕ/ψ angles of the polypeptide backbone and does not have interactions with the inhibitor.

Interactions with RP-TI and SP-TI. The crystal structures reported recently of *E. coli* EPSPS liganded with RP-TI and SP-TI (*25*) were included in this work for comparison. While the interaction of SP-TI with EPSPS was found to be similar to that of the genuine TI (Figure 5), the "wrong" diastereomer but much better inhibitor, RP-TI, induced substantial conformational changes in the enzyme's backbone and of active

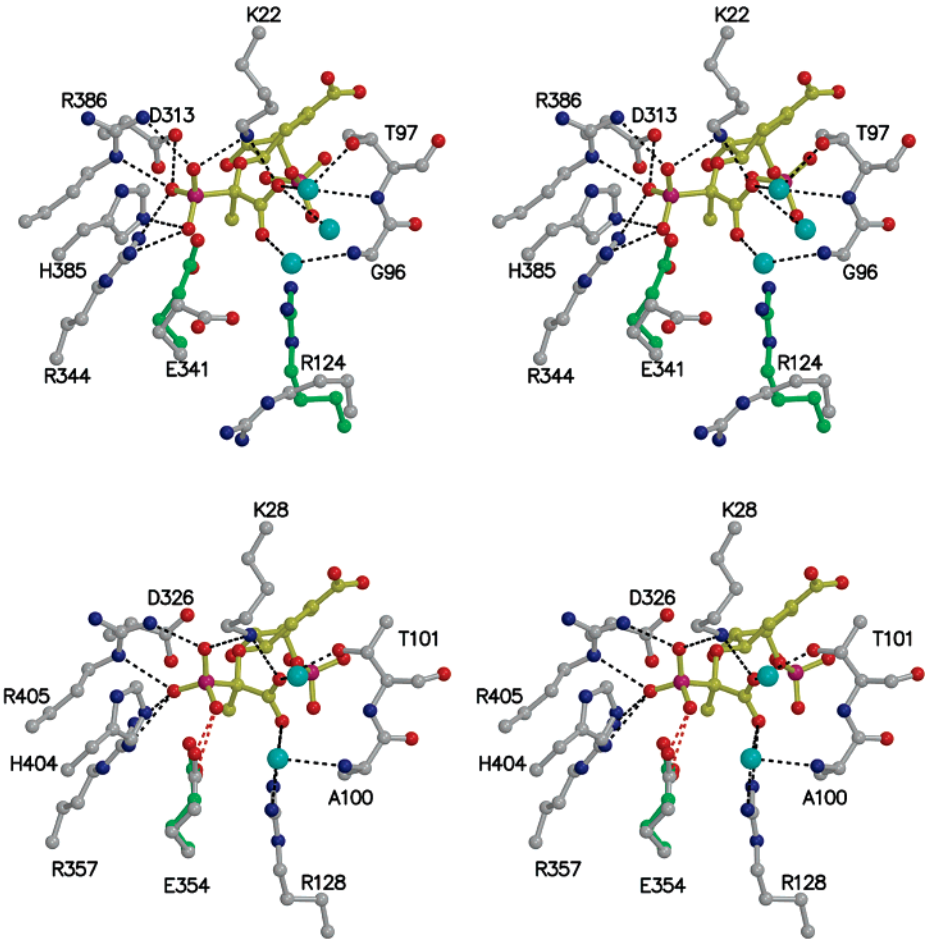

FIGURE 3: Interaction of RP-TI with EPSPS (stereoview). Top: RP-TI (shown in yellow) binding to *E. coli* EPSPS induces large conformational changes of the strictly conserved residues E341 and R124 (PDB code 1X8T; *25*). Bottom: RP-TI binding to CP4 EPSPS induces only a slight conformational change of E354 (=E341$^{E.coli}$), and R128 (=R124$^{E.coli}$) remains unaltered. The conformation of the RP-TI molecule is slightly different from that observed in the *E. coli* enzyme. The residues shown in green display the conformations found in the respective binary complexes with S3P. Black dotted lines indicate polar interactions; the red dotted lines in the CP4 enzyme indicate a steric clash between the RP-TI phosphonate moiety and Glu354. The cyan spheres denote water molecules.

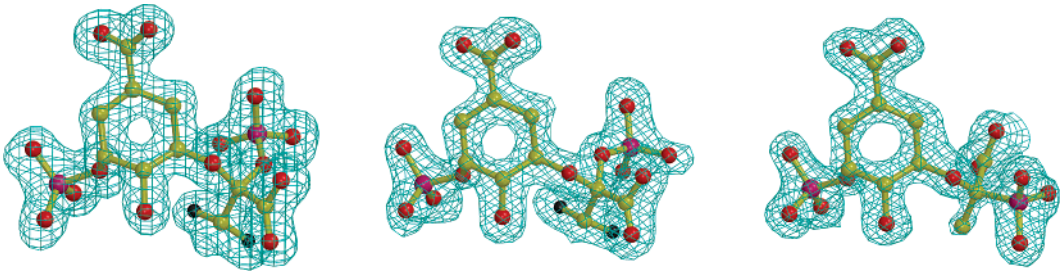

FIGURE 4: Structure determination of TI analogues bound to EPSPS. Displayed are the electron densities of the inhibitors, derived from $F_o - F_c$ Fourier syntheses and contoured at 3σ, omitting the model of 2F-TI in *E. coli* (left, 1.6 Å), 2F-TI in CP4 (middle, 1.8 Å), and RP-TI in CP4 (right, 1.6 Å) EPSPS after the last refinement cycle.

site residues. It was concluded that the enzyme's conformational flexibility enables efficient inhibitor binding.

Here, the CP4 enzyme was cocrystallized with RP-TI, and the structure was determined at 1.6 Å resolution (Table 1, Figures 3 and 4). In contrast to the *E. coli* enzyme, the structure of the CP4 enzyme remains essentially unaltered compared to the S3P-liganded CP4. In particular, the large conformational changes of the strictly conserved residues Glu354^{CP4} (=Glu341$^{E.coli}$) and Arg128^{CP4} (=Arg124$^{E.coli}$) observed in the *E. coli* EPSPS·RPTI complex do not occur in the CP4 EPSPS·RPTI structure. The Glu354^{CP4} side chain moves only slightly upon inhibitor binding, leaving an oxygen atom of the phosphonate group of RP-TI in close proximity to the carboxyl group of Glu354 (2.1 Å to the carboxyl oxygen and 3.0 Å to the carboxyl carbon atom); this could give rise to a steric clash, resulting in decreased binding efficiency. The guanidinium group of Arg128^{CP4} establishes a salt bridge with the carboxyl group of the inhibitor, an electrostatic interaction that does not exist in the *E. coli* EPSPS·RPTI complex. The Glu354 and Arg128 interactions with the inhibitor reflect the rigidity of the active site of CP4 EPSPS relative to the *E. coli* enzyme and apparently result in significant conformational change in the inhibitor molecule (Figure 3). Thermal denaturation studies indeed demonstrated that the CP4 enzyme is considerably more stable than the *E. coli* enzyme (*19*).

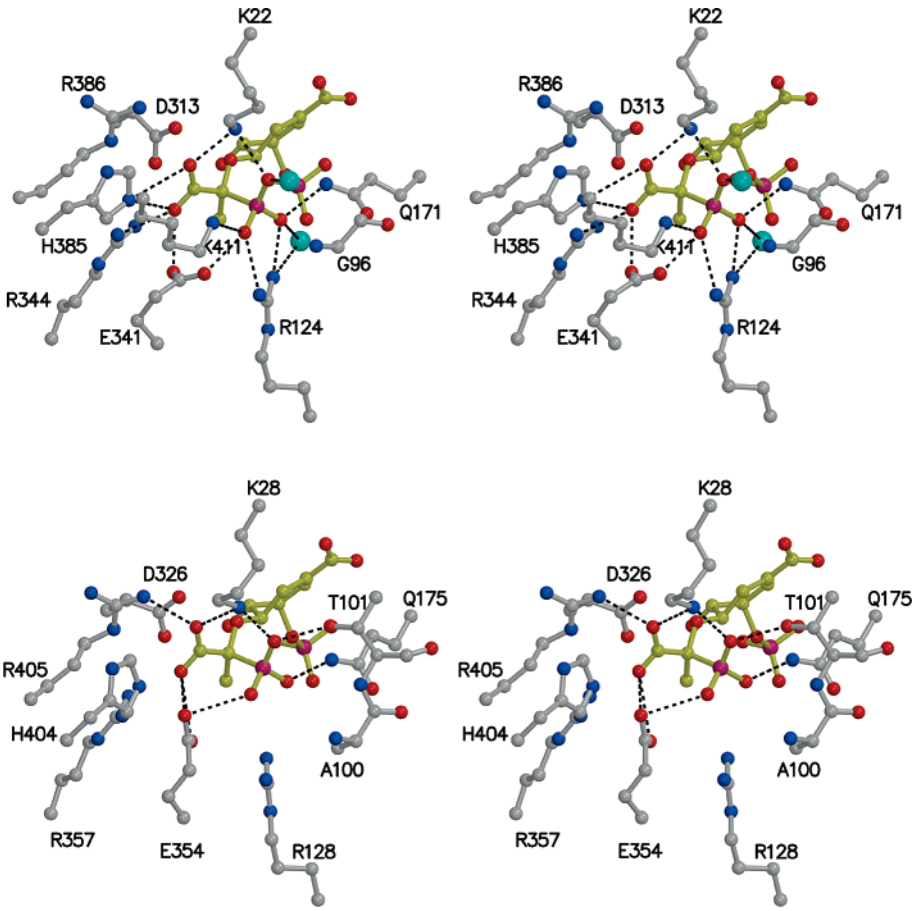

FIGURE 5: Interaction of the SP-TI with EPSPS (stereoview). Top: SP-TI (shown in yellow) binding to *E. coli* EPSPS is similar to that observed for the genuine TI (PDB code 1X8R; *25*). Bottom: Manual docking of the SP-TI molecule into the active site of CP4 indicates a loss of electrostatic interactions between the inhibitor molecule and residues Arg128 and His404. Black dotted lines indicate polar interactions. The cyan spheres denote water molecules.

Several cocrystallization trials of the CP4 enzyme liganded with SP-TI failed, presumably due to its poor binding affinity ($K_i = 76\ \mu M$). Manual docking of the SP-TI molecule from the *E. coli* enzyme (PDB code 1X8R) into the closed forms of the CP4 enzyme (i.e., the S3P-, 2F-TI-, and RP-TI-liganded structures) indicates that the distance between $Arg128^{CP4}$ and the inhibitor's phosphonate group is too large (>3.8 Å) to establish the (2.8 Å) salt bridge observed in the *E. coli* enzyme (Figure 5). In addition, the docking results indicate that the interaction between the carboxyl group of SP-TI and $His385^{E.coli}$ (2.9 Å) in the *E. coli* enzyme does not exist in the CP4 enzyme (distance 3.8 Å). The decreased electrostatic interactions between SP-TI and the CP4 enzyme may account for the decreased binding affinity of this inhibitor for CP4 EPSPS.

Alberg et al. determined that both 2F-TI ($K_i = 4$ nM) and RP-TI ($K_i = 15$ nM) are nanomolar-range inhibitors of *Petunia hybrida* EPSPS, and Priestman et al. determined that RP-TI exhibits similar potency against *E. coli* EPSPS ($K_i =$ 16 nM), demonstrating that select TI analogues constitute the most potent inhibitors of the EPSPS reaction (*11*, *24*, *25*). Molecular docking calculations based on the crystallographically determined structures of EPSPS·TI analogue complexes did not explain why RP-TI (the "wrong" diastereomer) is a much better inhibitor of EPSPS than SP-TI (*25*). Using the here-determined structures, we performed molecular docking studies, but the results were inconclusive and did not explain the differences in inhibitory potential of 2F-TI and RP-TI on the *E. coli* and CP4 enzymes, and these studies are therefore not included in this work. It appears that, for EPSPS, knowledge of the binding pattern of the TI analogues in the dead-end complexes is insufficient to explain the observed values for inhibitory potency. We conclude that the crystallographically determined structures reflect only part of the EPSPS interaction with inhibitors such as these TI analogues and thus do not reveal the complete molecular mode of inhibitor action.

It is known that the reaction of EPSPS follows an induced-fit mechanism (*19*, *23*); S3P binding induces global conformational changes from an open (ligand-free) to a closed (liganded) state. Like S3P, TI analogues initially will bind to the open state of the enzyme to form a "collision complex" (Figure 6), and the formation of the "dead-end inhibitor complex" will be completed upon the enzyme's transition to the closed state. For inhibition of *E. coli* EPSPS by RP-TI, it was proposed that events during these global structural changes may be altered as a result of the enzyme's initial interaction with the inhibitor (*25*). Furthermore, a change in the unimolecular rate constants that govern the open−closed transition to the dead-end complex would affect the inhibition constant, K_i. Here, we propose that the differential inhibition observed for the *E. coli*, *S. aureus*, and CP4 EPSPS may be due to alteration of the open−closed transition of these enzymes during catalysis and/or upon interaction with TI analogues. For example, the differences in the positions of the phosphonate/phosphate moieties of the TI analogues may

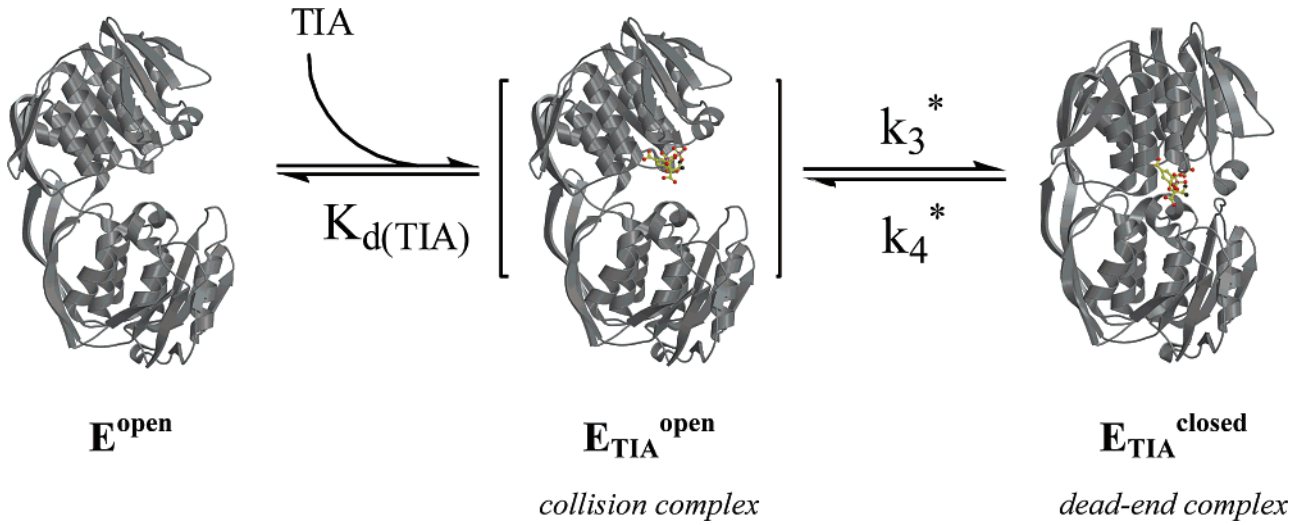

FIGURE 6: Proposed molecular mode of action of TI analogues on EPSPS. On the basis of the structural data available to date, TI analogues (TIAs) would initially interact with the open state of EPSPS to form a *collision complex*, determined by the dissociation constant $K_{d(TIA)}$, followed by an open−closed transition to the *dead-end complex*, determined by the rate constants k_3* and k_4*. Under the steady-state conditions applied here, the measured K_i values represent the K_d only if the ratio of k_3* and k_4* is not altered as a result of the inhibitor's interaction with the enzyme. The structures shown are that of the CP4 enzyme (left, open, PDB code 2GG4) interacting with 2F-TI, shown in yellow, to form the closed state (right, this work). The putative collision complex was modeled with 2F-TI bound to the open state of the enzyme after alignment of the N-terminal (top) globular domains of the open state and the closed states. It was previously suggested that S3P (and analogues thereof) would initially bind to the N-terminal domain of EPSPS (*35*).

influence the rate of the enzyme's conformational change to the closed, catalytically active state. Ligand binding to receptors has been shown to be strongly influenced by phosphate moieties, as demonstrated recently for triose phosphate isomerase and orotidine 5′-monophosphate decarboxylase (*35*, *36*). This hypothesis cannot be tested by steady-state kinetics and crystallography alone, but requires sophisticated kinetic experiments. The gross conformational changes that the enzyme undergoes have led to unreliable results from docking experiments, and this, together with the confined space and highly charged nature of the active site, has impeded the development of second-generation EPSPS inhibitors.

It is likely that the collision complexes of the respective inhibitors with both *E. coli* and CP4 EPSPS are formed with the low-energy states of the TI analogues. Presumably, these low-energy inhibitor conformations are preserved during the structural changes of the *E. coli* enzyme because large side chain and even backbone conformational changes effectively accommodate inhibitor binding. In contrast, the CP4 enzyme appears to be less flexible, and as a result, the TI analogues themselves must undergo structural changes. Notably, it was reported that glyphosate binds to the CP4 enzyme in a condensed, high-energy conformation that exhibits poor inhibitory properties (*19*). We therefore performed ab initio energy calculations of the different TI analogue conformers with GAMESS (*34*) (data not shown). Although the conformations of 2F-TI and RP-TI when bound to CP4 were predicted to be higher in energy than the conformers bound to the *E. coli* enzyme, the energy differences did not explain the differences in inhibitory properties.

CONCLUSIONS

Previous studies with EPSPS inhibitors other than glyphosate have utilized class I enzymes from *E. coli* or *P. hybrida*. It was assumed that reaction intermediate analogues would inhibit class II enzymes to the same or similar degree compared to class I enzymes. Our results reveal, however, that the class II EPSPS from CP4 and *S. aureus* are considerably less sensitive than *E. coli* EPSPS to inhibition by these TI analogues. These findings imply that the genuine tetrahedral intermediate states of class I and II enzyme reactions may differ considerably in conformation and energy. Such phenomena are typically not taken into account in designing TI analogues, because it is assumed that intermediate species adopt the same conformational states during the reaction, irrespective of the enzyme's genetic origin. Accumulated evidence demonstrates that many bacterial, fungal, and apicomplexan pathogens depend on EPSPS for pathogenicity and survival. Our studies indicate that such microorganisms are likely to exhibit tolerance to inhibitors developed on the basis of the well-understood kinetic and structural properties of *E. coli* EPSPS. Consequently, future efforts toward the discovery and design of EPSPS inhibitors with potential as broad-spectrum antibiotics should be performed using class II enzymes from pathogenic organisms.

ACKNOWLEDGMENT

We thank Krystle Gross-Roberts (University of Kansas) for research assistance.

SUPPORTING INFORMATION AVAILABLE

Figures S1−S5. This material is available free of charge via the Internet at http://pubs.acs.org.

REFERENCES

1. Bentley, R. (1990) The shikimate pathway—a metabolic tree with many branches, *Crit. Rev. Biochem. Mol. Biol. 25*, 307−384.
2. Haslam, E. (1993) *Shikimic Acid: Metabolism and Metabolites*, John Wiley & Sons, Chichester, U.K.
3. Kishore, G. M., and Shah, D. M. (1988) Amino acid biosynthesis inhibitors as herbicides, *Annu. Rev. Biochem. 57*, 627−663.
4. Buzzola, F. R., Barbagelata, M. S., Caccuri, R. L., and Sordelli, D. O. (2006) Attenuation and persistence of and ability to induce

protective immunity to a Staphylococcus aureus aroA mutant in mice, *Infect. Immun. 74*, 3498−506.
5. McDevitt, D., Payne, D. J., Holmes, D. J., and Rosenberg, M. (2002) Novel targets for the future development of antibacterial agents, *J. Appl. Microbiol. 92*, 28S−34S.
6. McArthur, J. D., West, N. P., Cole, J. N., Jungnitz, H., Guzman, C. A., Chin, J., Lehrbach, P. R., Djordjevic, S. P., and Walker, M. J. (2003) An aromatic amino acid auxotrophic mutant of Bordetella bronchiseptica is attenuated and immunogenic in a mouse model of infection, *FEMS Microbiol. Lett. 221*, 7−16.
7. Ferreras, J. A., Ryu, J.-S., Lello, F. D., Tan, D. S., and Quadri, L. E. N. (2005) Small-molecule inhibition of siderophore biosynthesis in Mycobacterium tuberculosis and Yersinia pestis, *Nat. Chem. Biol. 1*, 29−32.
8. Crosa, J. H., and Walsh, C. T. (2002) Genetics and assembly line enzymology of siderophore biosynthesis in bacteria, *Microbiol. Mol. Biol. Rev. 66*, 223−249.
9. Roberts, F., Roberts, C. W., Johnson, J. J., Kyle, D. E., Krell, T., Coggins, J. R., Coombs, G. H., Milhous, W. K., Tzipori, S., Ferguson, D. J., Chakrabarti, D., and McLeod, R. (1998) Evidence for the shikimate pathway in apicomplexan parasites, *Nature 393*, 801−805.
10. Steinrucken, H. C., and Amrhein, N. (1980) The herbicide glyphosate is a potent inhibitor of 5-enolpyruvyl- shikimic acid-3-phosphate synthase, *Biochem. Biophys. Res. Commun. 94*, 1207−1212.
11. Franz, J. E., Mao, M. K., and Sikorski, J. A. (1997) *Glyphosate: a unique global herbicide*, Vol. 189, American Chemical Society, Washington, DC.
12. Comai, L., Sen, L. C., and Stalker, D. M. (1983) An altered aroA gene product confers resistance to the herbicide glyphosate, *Science 221*, 370−371.
13. Stalker, D. M., Hiatt, W. R., and Comai, L. (1985) A single amino acid substitution in the enzyme 5-enolpyruvylshikimate-3- phosphate synthase confers resistance to the herbicide glyphosate, *J. Biol. Chem. 260*, 4724−4728.
14. Padgette, S. R., Re, D. B., Gasser, C. S., Eichholtz, D. A., Frazier, R. B., Hironaka, C. M., Levine, E. B., Shah, D. M., Fraley, R. T., and Kishore, G. M. (1991) Site-directed mutagenesis of a conserved region of the 5-enolpyruvylshikimate-3-phosphate synthase active site, *J. Biol. Chem. 266*, 22364−22369.
15. Eschenburg, S., Healy, M. L., Priestman, M. A., Lushington, G. H., and Schonbrunn, E. (2002) How the mutation glycine96 to alanine confers glyphosate insensitivity to 5-enolpyruvyl shikimate-3-phosphate synthase from *Escherichia coli*, *Planta 216*, 129−135.
16. Priestman, M. A., Funke, T., Singh, I. M., Crupper, S. S., and Schonbrunn, E. (2005) 5-Enolpyruvylshikimate-3-phosphate synthase from Staphylococcus aureus is insensitive to glyphosate, *FEBS Lett. 579*, 728−732.
17. Du, W., Wallis, N. G., Mazzulla, M. J., Chalker, A. F., Zhang, L., Liu, W. S., Kallender, H., and Payne, D. J. (2000) Characterization of Streptococcus pneumoniae 5-enolpyruvylshikimate 3- phosphate synthase and its activation by univalent cations, *Eur. J. Biochem. 267*, 222−227.
18. Barry, G. F., Kishore, G. M., and Padgette, S. R. (1992) Glyphosate tolerant 5-enolpyruvylshikimate-3-phosphate synthases, World Intellectual Property Organization International Publication Number WO 92/04449.
19. Funke, T., Han, H., Healy-Fried, M. L., Fischer, M., and Schoenbrunn, E. (2006) Molecular basis for the herbicide resistance of Roundup ready crops, *Proc. Natl. Acad. Sci. U.S.A. 103*, 13010−13015.
20. Eschenburg, S., Kabsch, W., Healy, M. L., and Schonbrunn, E. (2003) A new view of the mechanisms of UDP-N-acetylglucosamine enolpyruvyl transferase (MurA) and 5-enolpyruvylshikimate-3-phosphate synthase (AroA) derived from X-ray structures of their tetrahedral reaction intermediate states, *J. Biol. Chem. 278*, 49215−49222.
21. An, M., Maitra, U., Neidlein, U., and Bartlett, P. A. (2003) 5-Enolpyruvylshikimate 3-phosphate synthase: chemical synthesis of the tetrahedral intermediate and assignment of the stereochemical course of the enzymatic reaction, *J. Am. Chem. Soc. 125*, 12759−12767.
22. Boocock, M. R., and Coggins, J. R. (1983) Kinetics of 5-enolpyruvylshikimate-3-phosphate synthase inhibition by glyphosate, *FEBS Lett. 154*, 127−133.
23. Schonbrunn, E., Eschenburg, S., Shuttleworth, W. A., Schloss, J. V., Amrhein, N., Evans, J. N., and Kabsch, W. (2001) Interaction of the herbicide glyphosate with its target enzyme 5-enolpyruvylshikimate 3-phosphate synthase in atomic detail, *Proc. Natl. Acad. Sci. U.S.A. 98*, 1376−1380.
24. Alberg, D. G., Lauhon, C. T., Nyfeler, R., Fassler, A., and Bartlett, P. A. (1992) Inhibition of EPSP synthase by analogues of the tetrahedral intermediate and EPSP, *J. Am. Chem. Soc. 114*, 3535−3546.
25. Priestman, M. A., Healy, M. L., Becker, A., Alberg, D. G., Bartlett, P. A., Lushington, G. H., and Schonbrunn, E. (2005) The interaction of phosphonate analogs of the tetrahedral reaction intermediate with 5-enolpyruvylshikimate-3-phosphate synthase (EPSPS) in atomic detail, *Biochemistry 44*, 3241−3248.
26. Lanzetta, P. A., Alvarez, L. J., Reinach, P. S., and Candia, O. A. (1979) An improved assay for nanomole amounts of inorganic phosphate, *Anal. Biochem. 100*, 95−97.
27. Kabsch, W. (1993) Automatic procession of rotation diffraction data from crystals of initially unknown symmetry and cell constrants, *J. Appl. Crystallogr. 26*, 795−800.
28. Otwinowski, Z., and Minor, W. (1997) Processing of x-ray diffraction data collected in oscillation mode, *Methods Enzymol. 276*, 307−326.
29. Brünger, A. T., Adams, P. D., Clore, G. M., DeLano, W. L., Gros, P., Grosse-Kunstleve, R. W., Jiang, J. S., Kuszewski, J., Nilges, M., Pannu, N. S., Read, R. J., Rice, L. M., Simonson, T., and Warren, G. L. (1998) Crystallography & NMR system: A new software suite for macromolecular structure determination, *Acta Crystallogr., Sect. D: Biol. Crystallogr. 54*, 905−921.
30. Jones, T. A., Zou, J. Y., Cowan, S. W., and Kjeldgaard, M. (1991) Improved methods for building protein models in electron density maps and the location of errors in these models, *Acta Crystallogr., Sect. A 47*, 110−119.
31. Kraulis, P. J. (1991) MOLSCRIPT: a program to produce both detailed and schematic plots of protein structures, *J. Appl. Crystallogr. 24*, 946−950.
32. Esnouf, R. M. (1997) An extensively modified version of MolScript that includes greatly enhanced coloring capabilities, *J. Mol. Graphics Modell. 15*, 132−134.
33. Merrit, E. A., and Bacon, D. J. (1997) Raster3D: Photorealistic Molecular Graphics, *Methods Enzymol. 277*, 505−524.
34. Schmidt, M. W., Baldridge, K. K., Boatz, J. A., Elbert, S. T., Gordon, M. S., Jensen, J. H., Koseki, S., Matsunaga, N., Nguyen, K. A., Su, S., Windus, T. L., Dupuis, M., and Montgomery, J. A. J. (1993) General atomic and molecular electronic structure system, *J. Comput. Chem. 14*, 1347−1363.
35. Amyes, T. L. and Richard, J. P. (2007) Enzymatic catalysis of proton transfer at carbon: Activation of triosephosphate isomerase by phosphite dianion, *Biochemistry 46*, 5841−5854.
36. Amyes, T. L., Richard, J. P., and Tait, J. J. (2005) Activation of orotidine 5′-monophosphate decarboxylase by phosphite dianion: The whole substrate is the sum of two parts, *J. Am. Chem. Soc. 127*, 15708−15709.
37. Stauffer, M. E., Young, J. K., Helms, G. L., and Evans, J. N. (2001) Chemical shift mapping of shikimate-3-phosphate binding to the isolated N-terminal domain of 5-enolpyruvylshikimate-3-phosphate synthase, *FEBS Lett. 499*, 182−186.

BI701095U